High variability of microbial diversity from lampenflora of two bas-reliefs in the Pommery Champagne cellar

Stéphanie Eyssautier-Chuine, Ludovic Besaury, Nicolas Richet, Nathalie Vaillant-Gaveau, Sébastien Laratte, Marine Rondeau, Clément Pierlot, Alexandre Brunet, Maxime Gommeaux

High variability of microbial diversity from lampenflora of two bas-reliefs in the Pommery Champagne cellar

Stéphanie Eyssautier-Chuine[1*], Ludovic Besaury[2], Nicolas Richet[3], Nathalie Vaillant-Gaveau[3], Sébastien Laratte[1], Marine Rondeau[4], Clément Pierlot[4], Alexandre Brunet[1], Maxime Gommeaux[1].

[1] Université de Reims Champagne-Ardenne, GEGENAA, Reims, France
[2] Université de Reims Champagne Ardenne, INRAE, FARE, UMR A 614, Chaire AFERE, Reims, France.
[3] Université de Reims Champagne-Ardenne and INRAE, RIBP USC 1488, Reims, France.
[4] Vranken-Pommery Group, 5 Place du Général Gouraud, BP1049, 51689 Reims, cedex 2, France
[*] Email: stephanie.eyssautier@univ-reims.fr

Abstract

Pommery Champagne cellar has the originality to be in the underground of Reims city (NE - France) and has got monumental bas-reliefs carved in chalk walls. Bas-reliefs were illuminated for tourist visits and led to a lampenflora growth with different coloured areas which mar the beauty of the artworks. This study was focused on the characterization of the lampenflora of two bas-reliefs (named Fete de Bacchus and Silene) with the hypothesis that the different visual aspects of biofilms are associated to different phototrophic components. The goal was to control the proliferation of the lampenflora. Molecular analysis revealed distinct exogenous and opportunistic microorganisms in the two bas-reliefs though the bacteria:fungi ratio was remarkably constant. Pseudomonadota, Acidobacteriota, Bacteroidota and Actinomycetota were surprisingly dominant on Cyanobacteria. Bacchus had a higher microbial diversity than Silene. The different areas within Bacchus were composed of distinct communities while this was not the case for Silene. Phototrophs reflected specificity of each pit, Bacchus was mainly colonised by *Chromochloris* algae whereas Embryophyta and *Stichococcus* rather grew in Silene. The perspectives of this study are to propose a sustainable management of the cellar, notably the lighting strategy and visitor circuit, as well as preventive and curative treatments.

Key words

Lampenflora, microbial communities, DNA sequencing, subterranean site, Pommery Champagne cellar

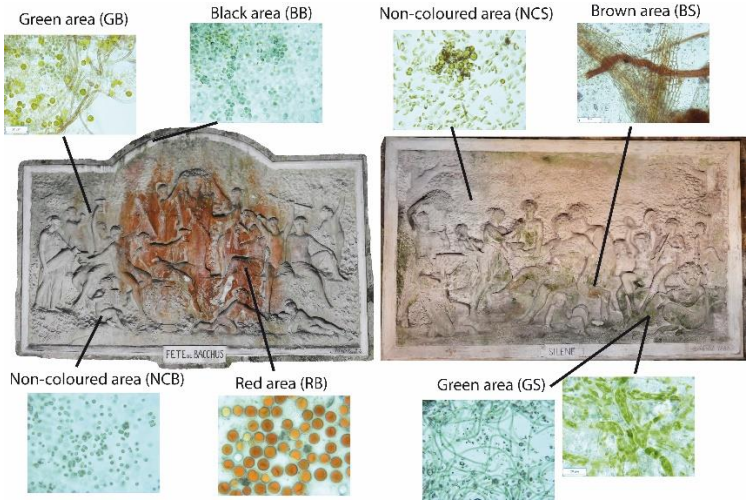

1. Introduction

The beauty and cultural significance of underground sites gave rise to a notable interest for tourist attraction. In contrast with brief scientific visits, the massive people influx required installation of walking paths and artificial lights. The consequence was to irreversibly alter the natural environmental conditions with an increasing of temperature and CO_2 level by visitors and air currents (Martin-Sanchez et al., 2014) which gave access to complex communities called lampenflora. Such biofilms replaced progressively the original microbiota as biovermiculations combining clayey sediments and microbial populations of oligotrophic cave environments composed of chemolithoautotrophic microorganisms (Tomczyk-Żak and Zielenkiewicz, 2016). The lampenflora is characterized by phototrophic organisms developed near lamps and at distances over 10 m (Mulec et al., 2012; Baquedano Estévez et al., 2019). Such biofilms are composed of colonizers from outdoor habitats selected according to their adaptability to new microclimatic conditions: no natural light, weaker aeration but increased humidity (Ariño et al., 2010) and an oligotrophic substrate but with organic matter provided by native communities (Addesso et al., 2021). Over time, the lampenflora usually gathers different microbes, aerophytic algae, cyanobacteria, bryophytes, mosses and ferns (Mulec and Kosi, 2009; D'Agostino et al., 2015; Duan et al., 2021). Despite the invasive and unsightly aspect, the lampenflora is sometimes considered as a part of the underground natural environment but it is also considered as biodeteriogens and can lead to irreversible damage when biofilms alter paintings and high-value geological formations (Bastian and Alabouvette, 2009; Saiz-Jimenez et al., 2011; Cennamo et al., 2016; Perez, 2018).

In the city of Reims located in the North-East of France, the basement made of chalk rock was quarried for building houses and monuments. Quarries were reused centuries later by winemakers to age Champagne wine from the 19th century, thanks to perfect environmental conditions: darkness, low variation of temperature and high humidity all over the year. They were listed as a UNESCO World Heritage site in 2015. The lampenflora clearly occurred on stone walls where the illumination was intensified especially on monumental bas-reliefs carved in the 19th century. These artworks were previously highlighted by incandescent lamps and in recent years by LED for tourist visits (180,000 people/year). Once lampenflora installed, recurring cleanings do not prevent its quick recolonisation causing spread discolorations which visually mar and physically degrade the artworks as some visible "scars" and stone replacement testify to the damage. Moreover, the lampenflora grows in spite of a current light control by a direct limited lighting time on the bas-reliefs but contemporary artworks exhibited in the cellar pits imply an indirect thus low irradiances on bas-reliefs but enough for the lampenflora growth (Albertano et al., 2003; Mulec et al., 2008).

The purpose of this study is (1) to characterize contrasted microbial communities as lampenflora which thrive on two monumental bas-reliefs of the cellar, named "Fete de Bacchus" and "Silene", (2) to test the hypothesis that the difference in the macroscopic aspect of the biofilms mainly corresponds to differences in the phototrophic component of the stone-colonizing communities (and thus, pigmented organisms) and (3) to get a better understanding of the parameters influencing biofilm development in cellars and caves that are open to the public and, in turn, helping to elaborate preventive and curative strategies, and suggesting a management reconciling heritage preservation with tourism exploitation in the cellar. This investigation and analyses were conducted to compare the different microbial communities developed on each bas-relief and communities between both bas-reliefs which are located in two different pits. We finally define the environmental origin of the microorganisms and their potential involvement in the stone biodeterioration.

This work started *in-situ* by sampling different areas detected by their colour and analysing by colourimetry, chlorophyll fluorescence and pH measurement. A laboratory investigation was carried out to quantify chlorophyll pigments, carotenoids and phycobiliproteins. Finally, the biodiversity of biofilm areas was analysed by means of optical microscopic observation of biofilm samples, cultivation and rRNA sequencing-based identification of isolates as well as Illumina-based high-throughput sequencing of 16S and 18S rRNA genes from biofilm-extracted DNA. Statistical and analyses were performed in order to correlate the different biological results with all the metadata associated.

2. Materials and methods

2.1. Description of the study sites and cleaning history of the bas-reliefs

The specificity of Pommery cellar is the monumental bas-reliefs carved in chalk rock between 1882 and 1885 by a French sculptor, Gustave Navlet. The lampenflora invaded bas-reliefs whose walls are always saturated of water, available resource for the microbial growth. Pits and galleries are at 30 m depth and were quarried in a fractured chalk, limestone with a high porosity (40.4 %) and a high water saturation (94.4 %) (Franco-Castillo et al., 2022). The temperature is from 14°C in winter up to 17°C in summer and a relative humidity from 95 to 99 %.

The cleaning frequency of the lampenflora varied according to the artwork and went from nil or once to three times between 2014-2023 and no other details before this period was listed by the stakeholders of the cellar. It was carried out by a commercial biocide or/and by carbonate air-scrub but a visual recolonization was observed after six months causing spread discolorations which visually mar the artwork. In addition, stone replacements are also observed by a clear difference in biocolonisation which suggests physical biodeterioration implications from the lampenflora over time and a restoration by repair compound varying from the original stone. Fete de Bacchus bas-relief was never cleaned so biofilms are growing for a long time, and Silene bas-relief has already been cleaned in 2014 by a commercial biocide and bicarbonate airbrushing.

2.1.1. Fete de Bacchus bas-relief

The bas-relief Fete de Bacchus (Bacchus) basement is at 4 m from the ground and dimensioned 5 m wide and 8 m high (Fig.S1a). The sculpture thickness is around 15-20 cm (Fig. 1) (Franco-Castillo et al. 2022). It is located on the south wall of a pyramid-shaped pit with a ground dimension around 10 x 12 m and 30 m high up to the outdoor ground from which a dim light comes from a glazed opening 2 m in diameter. In the pit, a spotlight is currently fixed on the wall on the opposite of the artwork at 6 m high to illuminate it (Fig. 2a). This light is turned on by a switch for a few minutes for visits which limits the light supply. Moreover, the Vranken-Pommery Domain creates an art exhibit every year with contemporary artworks in the different pits and galleries of the cellar (Experience Pommery #16). That induces lighting to illuminate them, and some artworks are luminous themselves. That is the case in Bacchus pit, where artworks are luminous, nevertheless the light intensity measured at different points on the bas-relief through the photosynthetically active radiation (PAR) is currently very low (0.1 µmol photons.m^{-2}.s^{-1}).

In-situ lampenflora observations clearly show regular non-colonised zones always located to the left of the statues where the red lampenflora is largely expanded (Fig. S2). Those zones suggest shadow zones where a lack of light prevented phototrophic microorganism development, since the light source came from the west wall of the pit. This orientation of the red lampenflora can be explained by the settlement of a large red and green luminous artwork in 2009 (Experience Pommery #6) which was hanged up on the west wall and probably fostered the growth of biofilms.

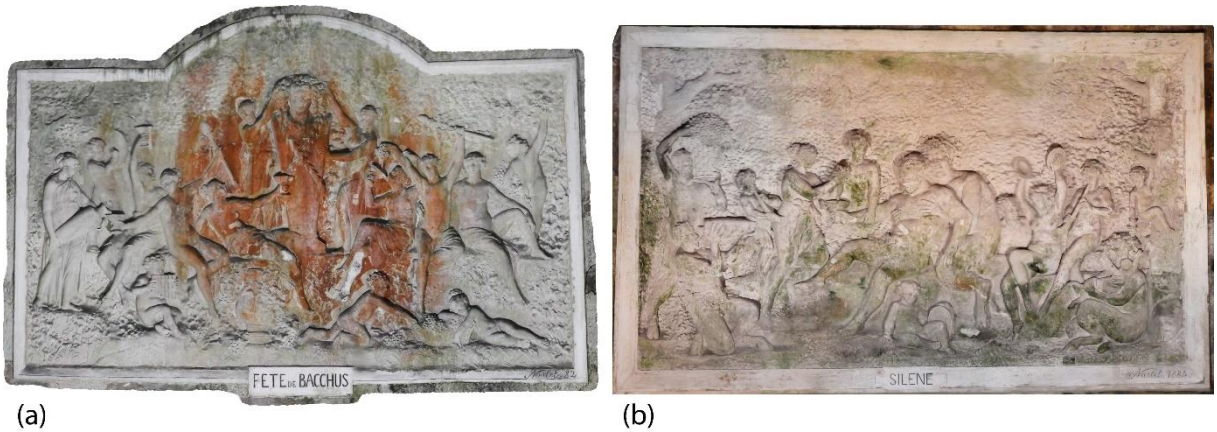

(a) (b)

Fig. 1. (a) Fete de Bacchus bas-relief (8 x 5 m) and (b) Silene bas-relief (15 x 6 m) carved in the chalk rock of two different pits in the Pommery Champagne cellar. Bacchus image was built by photogrammetry from 94 photos and Silene image from respectively 153 photos (Coolpix B700) by Agisoft Metashape v.1.7.2 software.

2.1.2. Silene bas-relief

Silene bas-relief is located at 3 m from the ground, and it is 15 m wide, 6 m high and inclined of 10° (Fig.S1b) and the sculpture thickness is around 25 cm (Fig. 1) (Franco-Castillo et al. 2022). The artwork was carved in the west wall of a pyramid shape pit. This pit is around 10 x 12 m to the ground and 30 m high up to the outdoor well which illuminate naturally the pit.

Artificial spotlights also illuminated the bas-relief, located on the lateral walls at 5 m high (1)-(2) and a third one is on the opposite wall of the bas-relief at 10 m high (3) (Fig. 2b). Nevertheless, the light intensity measured from the bas-relief is currently low (0.1 µmol photons.m^{-2}.s^{-1}) and the lighting time is limited to a few minutes like in Bacchus pit. Nevertheless, a ramp of 10 halogen spotlights settled at 2 m below the bas-relief, ran for several years but it is no longer operating now. However, the in-situ observations displayed a net lampenflora growing in the lower part of the artwork, closer to the spot ramp and in the highest part because of the inclination of the bas-relief, well exposed to the ramp (Fig. S3). Finally, a modern artwork is currently exposed in the middle of the pit and always lit by LED lights on the ground.

Fig. 2. Schematic map of the pits with bas-reliefs and current locations of spotlights.

2.2. Sampling and characterization of the lampenflora

2.2.1. Sampling method

The sampling was carried out from a visual selection of 7 coloured areas and non-coloured areas (Fig. S4-Table S1). Bacchus showed three coloured areas: the major and central red area (Red Bacchus- further referred to as RB), in the secondary and peripheral green area (Green Bacchus, GB), in the black

upper border of the bas-relief (Black Bacchus, BB) and finally in the peripheral non-coloured area (Non-Coloured Bacchus, NCB). Silene had two coloured areas: the major green area (Green Silene-GS) and a minor brown area (Brown Silene, BS), and a non-coloured area (Non-Coloured Silene, NCS). Every area was sampled by means of a scalpel cleaned with ethanol, samples were transferred into sterile tubes, and stored at 4 °C until analysis. For culture-based and molecular characterization of the biological diversity, in order to account for the small-scale variability, 8 to 10 replicate samples (150 ± 32 mg fresh weight) from each area were collected. The corresponding sampling surface was in the order of 1 cm² but not determined precisely. For pigment quantification, the biofilms were totally scraped and collected from two 5 x 5 cm zones from each area (1 for liposoluble pigments and 1 for phycobiliproteins).

2.2.2. Characterization of colonized and non-colonized areas on the bas-reliefs

2.2.2.1. Colourimetry

Colour change was performed with 10 measurements in a significative spot for each area with a Chroma Meter CR-400 from Konica-Minolta with a light projection tube CR-A33c of 11 mm diameter (corresponding to the measurement zone). Calibrations were previously performed with a white ceramic plate CR-A43. Values are given in the CIE-$L^*a^*b^*$ colour space (European committee for Standardization, 2011), with three dimensionless parameters determining the colour: L^* indicates lightness; a^* and b^* are the chromaticity coordinates. Then the average and the standard deviation were calculated.

2.2.2.2. Photosynthetic activity

Fifteen in-situ measurements were carried out on each area by means of a photosynthesis yield analyser, Junior PAM Chlorophyll Fluorometer (Walz, Effeltrich, Germany) comprising a pulse-amplitude modulation device (PAM) in combination with saturating pulse analysis of fluorescence quenching. It is a non-destructive technique for the characterization of phototrophic biofilms on substrates commonly employed now in cultural heritage (Miller et al., 2011; Bruno et al., 2019; Del Rosal et al., 2021). This handheld device was connected on one side to a laptop with WinControl-3 software (Walz) and on the other side to the studied area via a 50 cm long flexible fibre optic with 1.5 mm active diameter. Junior PAM released a blue power LED (460 nm) for pulse modulated fluorescence excitation and saturating pulses (1 s, 10 kHz) and collected chlorophyll *a* fluorescence emitted by phototrophic microorganisms especially algae.

Site conditions (artwork at several meters high) prevented from performing a dark-adaptation before measurements, thus the two recorded parameters were the minimal fluorescence of light-adapted biofilm (F_0') and the maximal fluorescence during the saturating light (F_M'). From those parameters, ϕ_{PSII} was calculated from $F_V'/F_M' = (F_M' - F_0')/F_M'$, it corresponds to the relative effective quantum yield of photochemical energy conversion at steady-state photosynthesis (Pfendler et al., 2018a; Eyssautier-Chuine et al., 2021). For each area defined previously, 15 measurements were carried out before sample collection, the average and standard deviation of ϕ_{PSII} were then calculated.

2.2.2.3. pH measurements

pH of biofilms was measured with the Pocket pH-meter, LAQUAtwin pH-11 from Horiba with pH 7.00 and 4.01 pH buffers. This devise requires a low sample volume (0.1 ml) by means of a flat electrode enabling accurate (± 0.1 pH) direct measurements of solid micro samples. Three measurements were carried out on the non-coloured areas (NCB-NCS) but only one measurement was done on biofilm areas because of the coloration of the electrode by liposoluble pigments.

2.2.3. Characterization of areas in laboratory

2.2.3.1. Liposoluble pigment concentrations

Lampenflora colour is partly related to photosynthetic microorganisms as algae and cyanobacteria that produce photosynthetic pigments. A square biofilm sample (5 x 5 cm) was scraped in each area (non-coloured and coloured), they were weighed and transferred into sterile tubes, then 10 ml of 80% acetone was added. Tubes were kept in the dark for 2 h at 4°C. After centrifugation at 4°C for 10 min at 2075 rpm (Beckman Coulter allegraX-15R centrifuge), the supernatant was taken and the absorbance measured with Genesys 10 uv Scanning spectrophotometer (Thermoscientific) at 646, 663, and 470 nm. The concentrations of chlorophyll a, b and carotenoids were calculated with the following equations (1) (Wellburn, 1994). Pigment concentrations per surface unit ($mg.m^{-2}$) were then calculated by multiplying the volume of the extracted solution (10 ml) and finally by dividing the surface of the sample (0.0025 m^2).

$$\begin{aligned} &\text{- [Chlorophyll } a\text{] } mg.l^{-1} = 12{,}21 \times A_{663} - 2{,}81 \times A_{646} = C_a \\ &\text{- [Chlorophyll } b\text{] } mg.l^{-1} = 20{,}13 \times A_{646} - 5{,}03 \times A_{663} = C_b \\ &\text{- [Carotenoids] } mg.l^{-1} = [1000 \times A_{470} - 3{,}27 \times C_a - 104 \times C_b] / 198 \end{aligned} \quad (1)$$

2.2.3.2. Concentration of phycobiliproteins

For phycobiliproteins (PBP) quantification, 5 x 5 cm biofilm samples were scraped with the same protocol as samples for liposoluble pigments. Then they were suspended in 5 ml of 0.01 M Na_2HPO_4 buffer, pH 7, 0.15 M NaCl. Disruption of cells were carried out on first by cycles of freezing (-80°C) - thawing (90°C) method. After light microscope examinations, red round cells in RB were still not lysed, the disruption of cells was then carried on by sonication in an ice bath at with Bioblock Scientific vibracell sonifier at 20 kHz ± 50 Hz, 40% amplitude for 5 min. Ten sonication pulses, alternated with a cooling period, were needed for complete cell disruption. Sonicates were centrifuged at 8000 g for 30 min and the optical density (OD) of the supernatant was measured at 562, 615 and 652 nm (Bruno and Valle, 2017). Finally, concentrations of the most well-known phycobiliproteins (Allophycocyanin : APC, Phycocyanin: PC, and Phycoerythrin: PE) were calculated from equations (2) (Bennett and Bogorad, 1973). PBP concentrations per surface unit ($mg.m^{-2}$) were calculated by multiplying the volume of the extracted solution (5 ml) then by dividing the surface of the sampled zone (0.0025 m^2).

$$\begin{aligned} PC &= [A615 - 0.474\ (A652)]/5.34 \\ APC &= [A652 - 0.208\ (A615)]/5.09 \\ PE &= [A562 - 2.41\ (PC) - 0.849\ (APC)]/9.62 \end{aligned} \quad (2)$$

2.3. Microbial diversity

2.3.1. Isolation of strains by culture-based techniques

Isolation of bacterial, fungal, and phototrophic strains was performed to characterize the diversity of cultivable microorganisms present in the biofilms. One sample per area was suspended in 10 ml of distilled water and diluted from 10^0 to 10^{-5}. Then 100 µl of each dilution was inoculated on duplicate Petri dishes containing agar medium with Luria Bertani medium at 1/10 concentration (LB10) for bacterial isolation (Ezraty et al., 2014), Malt medium for fungal and yeast isolation (Sarkar et al., 2009) and Hoagland medium for phototroph isolation (Salamah et al., 2019) (Table S2). Cultures were maintained at 20 °C, 80% relative humidity and included an 12/12 light/dark period with by means of two neon lights (Sylvania Gro-Lux) with a photosynthetically active radiation (PAR) of 25 µmol $photons.m^{-2}.s^{-1}$. Microbial growth was monitored every week by binocular magnifier observations to isolate every strain time after time.

2.3.2. Identification of microbial strains

Strains were isolated from a morphological description. Bacterial DNA extraction was performed using Bacterial Genomic DNA kit from GenElute, fungi and yeast DNA was extracted with Plant/fungi DNA isolation kit from Norgen Biotek corp. and eukaryotic phototroph DNA with DNeasy PowerBiofilm from

Qiagen. DNA concentration and quality were determined by NanoDrop One UV-visible spectrophotometer (ThermoFisher).

Prokaryotic 16S and eucaryotic 18S rRNA genes were amplified by polymerase chain reaction (PCR), using specific primers (Eurogentec - Belgium): 8F (5'- AGAGTTTGATCCTGGCTCAG-3') and 1391R (5'-GACGGGCGGTGTGTRCA-3') for bacteria, NS1F (5'-GTAGTCATATGCTTGTCTC-3') and NS8R (5'-TCCGCAGGTTCACCTACGGA-3') for fungi and yeast, *rbcL* primers for algae and plants with S1F (5'-ATGTCACCACAAACAGAGACTAAAGC-3') and S1R (5'-GAAACGGTCTCTCCAACGCAT-3') . PCR reactions were carried out in 200 µl PCR tubes with a reaction volume of 50 µl: 41.25 µl of sterile ultra-pure H_2O (Millipore Milli-Q Water System), 5 µl of PCR buffer (Promega, France), 1 µl of dNTP (Promega, France), 1 µl forward primer, 1 µl reverse primer, 0.25 µl Go taq Polymerase (Promega, France) and 0.5 µl template DNA.

For the qualitative analysis, the amplified PCR products were checked by migration of a 5 µl of the PCR product on 1 % agarose gel electrophoresis (0.5 M TAE Buffer) before commercial Sanger sequencing (Genoscreen, France). The nucleotide sequences were aligned with the closest relative sequences of representatives in the GenBank database by BLASTN (Basic Local Alignment Search Tool), an algorithm using the CLUSTALW program (Thompson et al., 2002), available at NCBI (National Center for Biotechnology Information). Sequences were then deposited in the NCBI Genbank database under accession numbers listed in tables S5-S6.

2.3.3. Molecular analysis of the microbial community diversity in biofilm samples

The total microbial DNA was extracted with DNeasy PowerBiofilm (Qiagen) from 4 samples for each non-coloured and coloured area on the bas-reliefs. The DNA quality was determined by NanoDrop One UV-visible spectrophotometer (ThermoFisher) and 3 samples per area were sent to Integrated Microbiome Resource (IMR) at Dalhousie University in Halifax (Canada) for ILLUMINA MiSeq-based high-throughput sequencing, with primer pairs B969F (5' ACGCGHNRAACCTTACC 3') and BA1406R (5' ACG GGC RGT GWG TRC AA 3') for bacteria (Comeau 2011), and E572F (5' CYG CGG TAA TTC CAG CTC 3') and E1009R (5'AYG GTA TCT RAT CRT CTT YG 3') for eukaryota (Comeau et al., 2011). Sequencing data were processed using the Mothur software (Schloss et al., 2009). Operational taxonomic units (OTUs) were defined at 3% dissimilarity threshold using the opticlust algorithm (Westcott and Schloss, 2017), abundance tables and Alpha diversity indices were produced by Mothur at the phylum level and at the genus level. Corresponding data were plotted with the software R (see below) and Excel. Non-metric multidimensional scaling (NMDS) and analysis of molecular variance (AMOVA) on the Bray-Curtis inter-sample distance matrix were performed using Mothur.

The unprocessed sequencing read dataset has been deposited in the NCBI Sequence Read Archive (SRA) and is freely available under accession number PRJNA1045856 (https://www.ncbi.nlm.nih.gov/sra/PRJNA1045856).

2.3.4. Quantitative PCR

Fungal 18S and bacterial 16S rRNA gene copy numbers were determined by quantitative PCR (qPCR) amplification of biofilm extracted DNA from three or four samples per area, using the primers FR1 (5' AIC CAT TCA ATC GGT AIT 3') and FF390 (5' CGA TAA CGA ACG AGA CCT 3'), and 341F (5' CCT ACG GGA GGC AGC AG 3') and 515R (5' ATT ACC GCG GCT GCT GGC A 3') respectively (Lienhard et al., 2013). Genomic DNA of a cultivated fungal strain and a cultivated bacterial strain were amplified by PCR using the previous primers and diluted to serve as a standard range from 10^3 to 10^8 copies/µl. qPCR runs were performed on a Bio-rad CFX thermal cycler using ABsolute Blue QPCR Mix (ThermoFisher) and bacteriophage T4 gene 32 protein (New England Biolabs) as anti-inhibitor. After 15 min at 95 °C for enzyme activation, 40 cycles comprised 10 s at 95°C for denaturation, 45 s at 60°C for annealing and extension. The melt curve was performed from 65°C to 95°C, for 1 s at each 0.5°C. Raw results were processed using the software CFX Manager 3.1 (Bio-rad) before statistical analysis.

2.4. Statistical analysis

Multivariate statistical analyses were carried out with R.4.2.1 software (R Core Team, 2023) for graphics were produced with ggplot2 package (Wickham, 2009). For qPCR, XLSTAT was used for ANOVA test (checking the normality of the data distribution) then Fisher test (LSD).

3. Results

3.1. Colour measurements

Several different areas have been defined and characterized according to their colour (Table S3). On Bacchus, NCB was a clear yellowish stone area with high L^* of 83.4 and b^* of 12.2. Data were compared to dry and water saturated chalk colour and displayed that NCB L^* was between L^* of dry and saturated chalk and a^* and b^* were similar to the same parameters of the saturated chalk. Consequently, NCB was close to a saturated chalk. (RB was characterized by a red-orange colour of RB (a^* of 25.3 and b^* of 32.4). The green and black areas (GB and BB) had the same b^* with respectively 19.9 and 19.1 that displayed a yellow part in both biofilm areas. The parameter a^* was negative for GB (-4.2) and for BB (-5.8) which revealed a greening for both and more intense for BB. Moreover, L* was darker for BB with 44.3 than GB with 57.9. Therefore, colour data showed that BB was rather dark green.

Silene bas-relief had a non-coloured area whom the colour was characterized by L^* of 70.8 which was darker than the dry and water saturated chalk. Moreover, b* was at 16.0 which is more yellow than NCB and the saturated chalk. The darkening and yellowing of NCS were probably not associated to the water content in the stone but to a colonization which had not been detected to the naked eye. The green area (GS) had a L^* of 31.2, a^* of -7.4 and b^* of 11.4; all parameters are lower than GB and BB, especially much darker and greener. The brown area (BS) was characterized by L^* of 44.9 which was similar to RB and BB, a^* of 7.7 and b^* of 22.9 that corroborated the brown colour with much less red colour than RB.

Accordingly, the colour analysis could specify that GB was characterized by a low L* and a* thus green and dark colour which intensified in BB. RB had a low L*, a high a* and b* so it was a dark red-orange colour. NCB was characterized by a high L* thus a clear white colour probably associated to the water content in the stone whereas NCS on Silene had a weaker L* showing a darker stone than a water saturated stone. BS was characterized by a weak L* and a high b* so a dark yellow colour and GS had the weakest L* and a* thus it was a dark green area, darker than GB and BB.

3.2. pH measurements

On Bacchus bas-relief, pH of NCB was 8.6 thus basic (Table S3). BB and GB had respectively a pH of 8.3 and 7.5, therefore the pH remained basic but was lower than for NCB. On Silene bas-relief, NCS pH was neutral (7.1) and lower than NCB and GS had a pH at 7.4 and BS at 6.8. Consequently, areas on Silene had neutral to slightly acid pH whereas on Bacchus, areas were basic. Nonetheless, green area pH on both bas-reliefs were similar.

3.3. Liposoluble pigment concentrations

The characterization of Bacchus areas showed that chlorophyll *a* concentrations (chl.a) increased progressively between NCB, GB and BB with 0.77, 1.79 and 4.16 $mg.m^{-2}$ while RB chl.a was much lower at 0.41 $mg.m^{-2}$ (Table S4). NCB chl.b was 1.05 $mg.m^{-2}$ surprisingly higher than GB which chl.b was 0.70 $mg.m^{-2}$ whereas GB was greener than NCB. BB chl.b was the highest with 3.52 $mg.m^{-2}$. RB chl.b was also low at 0.36 $mg.m^{-2}$. Carotenoid concentrations displayed the same trend as chl.a with an increase between NCB, GB and BB (0.12, 0.99 and 5.49 $mg.m^{-2}$). RB carotenoids were high with 4.55 $mg.m^{-2}$. Accordingly, RB was characterized by a high concentration of carotenoids while chl. a and b were low. NCB area which is visually non-coloured, had low concentrations of the three pigments. Contrarily, all pigments in BB had high concentrations and GB had intermediate values between NCB and BB.

On Silene bas-relief, NCS displayed weak contents of pigments with respectively 0.83, 0.64 and 0.15 $mg.m^{-2}$ for chl.a, chl.b and carotenoids. GS was characterized by the highest chl.a concentration with 16.55 $mg.m^{-2}$, a high chl.b which was at 6.77 $mg.m^{-2}$ and carotenoids at 2.01 $mg.m^{-2}$. Finally, BS had

4.37 mg.m^{-2} lower than chl.a GS but similar to BB, chl.b was at 2.30 mg.m^{-2} and carotenoids were surprisingly low with 1.02 mg.m^{-2} that suggested the brown colour of this area did not result from those pigments.

3.4. Photosynthetic activity

On Bacchus, the relative quantum yield of the photosystem II varied from 0.30 for NCB and 0.31 for GB to 0.44 on RB (Table S4). On Silene, NCS GB ϕ_{PSII} was 0.39 so higher than NCB which had the same visual aspect whereas GS ϕ_{PSII} was higher with 0.43. On BS with brown colour, the chl. fluorescence was 0.35.

3.5. Phycobiliprotein concentrations

On Bacchus, phycobiliprotein (PBP) concentrations varied in function of the areas, RB had the highest values for the three measured PBP with a maximum of 7.32 mg.m^{-2} for APC while NCB had low contents for all PBP (Table S4). On Silene, the green area (GS) had the highest concentrations (5.52 mg.m^{-2}) though lower than RB on Bacchus. In addition, in both sites and all areas, allophycocyanin (APC) were higher than PC or PE concentrations.

3.6. Microbial diversity identified by high-throughput sequencing

3.6.1. Bacterial diversity

The number of 16S rRNA raw sequencing reads for the 22 samples was 1,457,140 but two samples had to be deleted due to poor quality (one replicate of NCS and one replicate of RB). After all quality control steps, the number of high-quality 16S rRNA reads was 1,233,252 in total and was between 12,197 (RB4) and 127,453 (BS4) per sample. At the threshold of 3% of dissimilarity, these reads were clustered into 10,621 OTUs. Seventeen OTUs comprised more than 1% of the total reads each, the largest OTU comprising 46,489 sequences, i.e. 3.8 % of the total reads. Contrarily, 58 % of the OTUs comprised only one read. After sub-sampling randomly each sample down to 12,197 reads, 4,360 OTUs were present. Fourteen OTUs comprised more than 1 % of the total reads each, the largest OTU comprising 9,844 sequences, i.e. 4.0 % of the total reads. Contrarily, 48 % of the OTUs comprised only one read.

The rarefaction curves (Fig. S5) did not reach a plateau suggesting that 16S sequencing depth did not enable to saturate the microbial diversity in the samples.

The observed community richness (number of OTUs per sample, S_{obs}) ranged from 239 to 1,093 (Table 1). S_{obs} was lower for GS samples and higher for BB samples. As a whole, Silene samples had lower S_{obs} than Bacchus samples, which was also the case for the Shannon diversity index. Furthermore, Good's coverage index values were lower for Bacchus samples than for Silene samples, suggesting that the Bacchus samples have a total diversity even higher than observed. The Chao1 richness estimator values suggested that for every sample, the total richness was 1.4-2.6 times as high as the observed richness (Chao1 divided by S_{obs}).

In Bacchus, BB had a higher richness and diversity than the other areas; on the opposite, RB had a poorer richness and diversity. In Silene, BS had a higher richness and diversity compared to NCS and GS.

The non-metric multidimensional scaling (NMDS) plot based on the OTU distribution table (Fig. S6a) indicated a clear difference between Bacchus and Silene biofilms, and within each bas-relief a clear grouping of the replicates of all areas defined for the Bacchus bas-relief though only for the NCS for the Silene bas-relief. AMOVA performed on the OTU distribution table confirmed the significant difference between the overall Silene and Bacchus bacterial diversities (Bonferroni p-value < 0.001), that was observed on the NMDS plot. AMOVA revealed significant differences between the 4 types of biofilm defined on the Bacchus bas-relief ($p < 0.001$) as well as between the 3 types of biofilm defined on the Silene bas-relief ($p = 0.028$). More specifically, among all possible pairs, AMOVA revealed significant differences between Non-Coloured Bacchus and either Black Bacchus ($p = 0.031$), Green Bacchus ($p = 0.024$), Brown Silene ($p = 0.024$) or Green Silene ($p = 0.029$).

Bas-relief	Samples	S_{obs}	Chao 1	Shannon	Coverage
Bacchus	NCB1	591	892	4.56	0.981
	NCB2	611	1145	4.46	0.978
	NCB3	552	905	4.63	0.983
	NCB4	494	749	4.41	0.985
	BB1	803	1388	4.92	0.972
	BB2	743	1267	4.51	0.974
	BB4	1093	2460	4.87	0.952
	RB3	426	631	4.00	0.988
	RB4	412	580	3.80	0.988
	GB1	545	854	3.94	0.981
	GB3	591	1085	4.04	0.977
	GB4	706	1855	4.28	0.968
Silene	NCS1	338	486	3.83	0.991
	NCS2	396	798	3.95	0.986
	BS1	369	683	4.07	0.987
	BS2	451	1069	4.18	0.980
	BS4	311	550	3.78	0.990
	GS1	372	620	4.32	0.989
	GS3	239	440	3.70	0.993
	GS4	321	483	3.88	0.991

Table 1. Alpha diversity indices of samples from bas-relief areas, calculated from the bacterial OTU abundance table. S_{obs} is the observed richness, Chao1 is the Chao1 richness estimator, Shannon is the Shannon diversity index, Coverage is Good's coverage index.

After taxonomic affiliation of the OTUs, only phyla representing more than 0.5 % of the total sequence reads for each area were further considered (Fig. 3). As a result, 14 main phyla of *Bacteria* dominated the microbial communities (8 phyla were under 0.5 %). The major phylum was *Pseudomonadota,* it was represented by a relative abundance between 31 % for BB4 and 73 % for RB4 in Bacchus and between 36 % for GS1 and 70 % for GS4 in Silene. In both bas-reliefs, the other main phyla were Bacteroidota with a maximum abundance (35 % for GB1), Acidobacteriota (22 % for GS1), Actinomycetota (23 % for NCS1), Chloroflexota (14 % for BB4), Gemmatimonadestes, Chlamydiota, Planctomycetota, Cyanobacteria, Dependentiae, Bacillota, Nitrospirota, Verrucomicrobiota, and Latescibacteria (Oren and Garrity, 2021).

Not all OTUs could be classified at the genus level. On Bacchus, NCB samples had a homogeneous diversity in genera (Fig. S7) with a majority of OTUs classified as *Hyphomicrobium*, *Dongia*, *Pseudonocardia* but also unclassified *Gemmatimonadaceae* and subgroup 6 (*Acidobacteriota*). BB samples had a majority of OTUs classified as unclassified *Microscillaceae, SWB02* (Hyphomonadaceae), *Bryobacter* or *Dongia* but also *Gemmatimonadaceae, Ardenticatenaceae*. RB samples had a majority of OTUs classified as *Hirschia* but also unclassified *Blastocatellaceae, Gemmatimonadaceae* and, for RB4, Xanthomonadales. Although three GB samples were clustered on the NMDS plot, the predominant groups were not the same for them, with a majority of OTUs classified as *Chitinophagaceae* for GB1, *Dongia* and *Microscillaceae* for GB3 and *Hyphomonadaceae* for GB4.

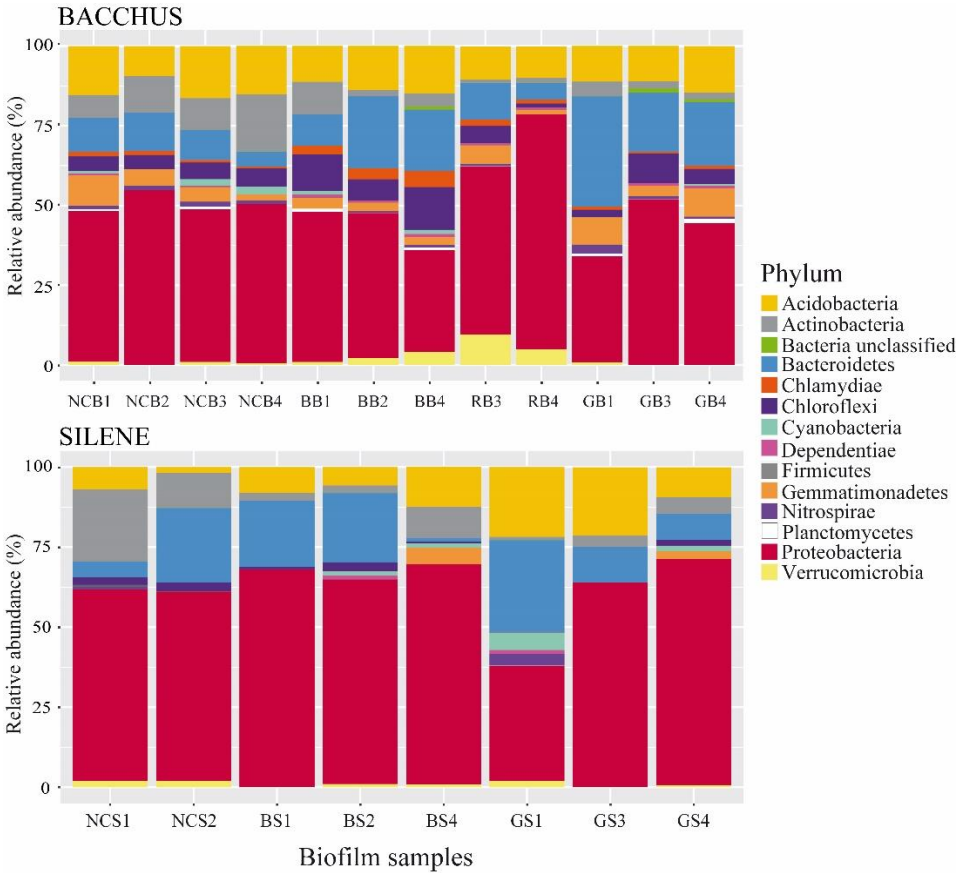

Fig. 3. Bacterial diversity at phylum level in Bacchus and Silene areas determined by Illumina-based high-throughput sequencing. Only the phyla representing more than 0.5 % of total sequences were considered.

On Silene areas, NCS samples displayed the same major OTUs with unclassified *Rhizobiaceae*, *Hyphomicrobium, Pseudonocardia*. Then BS and GS displayed a heterogeneity in the genera diversity, BS samples had not clear predominant groups, BS1 had *Pseudominobacter*, *Bryobacter*, unclassified *Rhizobiaceae*, BS2 rather had unclassified *Rhizobiaceae* and *Microscillaceae*, BS4 had *Hyphomicrobium*, unclassified *Hyphomonadaceae* and *Blastocatellia*. Finally, GS showed 3 samples without main OTUs, GS1 had *Bryobacter* and *Stenotrophobacter*, GS3 had unclassified *Blastocatellaceae* and *Shingomonadaceae*, GS4 had unclassified *Microscillaceae* and *Gemmatimonadaceae*.

Cyanobacteria displayed 7 genera. On Bacchus, *Chalicogloea* was the genus in all GB samples, representing 0.1 to 1.3 % of bacteria. They were comprised between 0.2 and 1.0 % in BB samples and 0.7 % in NCB1. Oxyphotobacteria_ofg were the vast majority of Cyanobacteria in NCB3 (1.8 %) and NCB4 (2.3 %), they were also present though less abundant lower in RB samples 0.02 % in RB4, RB3, NCB1 and GB4. RB3 sample was also characterized by Obscuribacterales_fg (0.02 %) and RB4 by *Chloroplast* (0.03 %). *Leptolyngbya* were only present in all BB samples, representing 0.05 to 0.2 % of bacteria. On Silene, *Chloroplast* were the only Cyanobacteria genus in NCS2 (0.02 %) and were in majority in NCS1. BS samples had Oxyphotobacteria_ofg as the main Cyanobacteria genus (with 1.0 and 1.2 %) except in BS1 which was different with *Chloroplast* (0.06 %) and *Leptolyngbya* (0.1 %). Finally in GS samples, *Leptolyngbya* was the main genus in GS1 (5.3 %) whereas *Chalicogloea* were in majority in GS3 0.3 %) and GS4 (0.4 %).

3.6.2. Eukaryotic diversity

The 18S rRNA gene sequence dataset was of poor quality. The number of raw sequencing reads for the 22 samples was 34,690 but 8 samples had to be deleted due to an excessively low number of high-quality sequences (1 replicate of each of BB-NCB-NCS, two replicates of GB and all three replicates of RB). After all quality control steps, the number of high-quality 18S rRNA reads was 26,842 in total and

was between 154 and 6,361 per sample. Sequences affiliated to animal phyla (Annelida, Arthropoda, Rotifera), representing 16 % of the total sequence set, were removed for further analysis, resulting in a total number of sequence reads for eukaryotic phototrophs and fungi of 22,259, and between 112 and 6,305 per sample. At the threshold of 3 % of dissimilarity, these reads were clustered into 693 OTUs. Twelve OTUs comprised more than 1 % of the total reads each, the largest OTU comprising 8,893 sequences, i.e. 40 % of the total reads. Contrarily, 78 % of the OTUs comprised only one read. Contrary to the 16S, the 18S data set was subsampled only for the calculation of the diversity indices and not for the NMDS and AMOVA in order not to obtain an excessively low number of reads for all samples.

The NMDS plot based on the OTU distribution table (Fig. S6b) indicated a difference between Bacchus and Silene biofilms, but within each bas-relief, no clear grouping of samples from the defined zones. AMOVA performed on the OTU distribution table confirmed the significant difference between the overall Silene and Bacchus fungal and phototrophic diversities (Bonferroni p-value = 0.007), that was observed on the NMDS plot. AMOVA revealed significant differences between the 3 types of biofilm defined on the Bacchus bas-relief ($p < 0.047$) but no significant differences between the 3 types of biofilm defined on the Silene bas-relief.

On Bacchus, Chlorophyta were the major phylum for the NCB1 and NCB4 samples with respectively 60 % and 67 % (Fig. 4) whereas they accounted only for 9 % and 43 % of reads for NCB2 and NCB3, respectively (50 % of reads being unclassified at the phylum level).
Muromycota represented 24 % of reads in NCB4, Ascomycota and Basidiomycota represented 20 % and 10 % of reads in NCB2, respectively. BB seemed the most homogeneous area, whose samples were characterised by Phragmoplastophyta as the major phylum (57 % in BB1, 64 % in BB2 and 87 % in BB4), then by unclassified Eukaryota (9 to 29 %), Ascomycota (9 % in BB1), Mucoromycota (3 % in BB4) and Basidiomycota. GB samples displayed a majority of reads unclassified at the phylum level (46, 81 and 58 % in GB1, GB3 and GB4, respectively). Then Chlorophyta ph. represented 31 % of reads in GB4 and Ascomycota 27 % in GB1. Finally, RB3 had a majority of Chlorophyta (62 %) and reads unclassified at the phylum level (37 %).
On Silene, NCS1 and NCS2 were different, NCS1 had 86 % of Chlorophyta and 13 % of Ascomycota whereas NCS2 had 81 % of Ascomycota and only 15 % of Chlorophyta. BS samples seemed homogeneous, dominated by Phragmoplastophyta (between 34 and 42 % of reads), Ascomycota (between 26 and 38 % of reads), 15 to 32 % of reads being unclassified at the phylum level. Chlorophyta represented 23 % of reads in BS1, compared to 1 % in BS2 and BS4. GS samples showed a high abundance of Phragmoplastophyta (92 % in GS4 and 48 % in GS1) whereas Chlorophyta dominated in GS3 (68 %). Ascomycota were also present at 27 % in GS1.
More details were disclosed at a genus level (Fig. S8). *Chromochloris* (Chlorophyta) were dominant in all NCB samples (between 36 and 49 %) except in NCB2 (2%), *Stichococcus* representing between 1 and 16 %. In NCB4, *Mortierella* represented 24 % of reads. *Chromochloris* were also in majority in RB3 (85 %). In BB samples, reads of *Embryophyta* unclassified at the genus level were dominant (between 49 and 85 %). In GB samples, *Chromochloris* represented 25% of reads in GB4, though a majority of reads were unclassified at the genus level. In GB1, *Calcarisporiella* and *Mortierella* represented respectively 17 and 13 %.
On Silene, NCS samples differed from one another, with a majority of *Stichococcus* (83 %) in NCS1 and *Plectosphaerella* (52 %) in NCS2. BS samples were dominated by *Embryophyta* reads unclassified at the genus level (29 to 37 %) but *Eukaryota* reads unclassified at the phylum level were abundant in BS4. Reads of *Hypocreales* unclassified at the genus level represented at 21 and 27 % for BS1 and BS2. *Stichococcus* represented 23 % of reads in BS1. Finally, GS1 and GS4 were dominated by unclassified Embryophyta (48 and 92 %) whereas GS3 was dominated by *Stichococcus* (63 %).

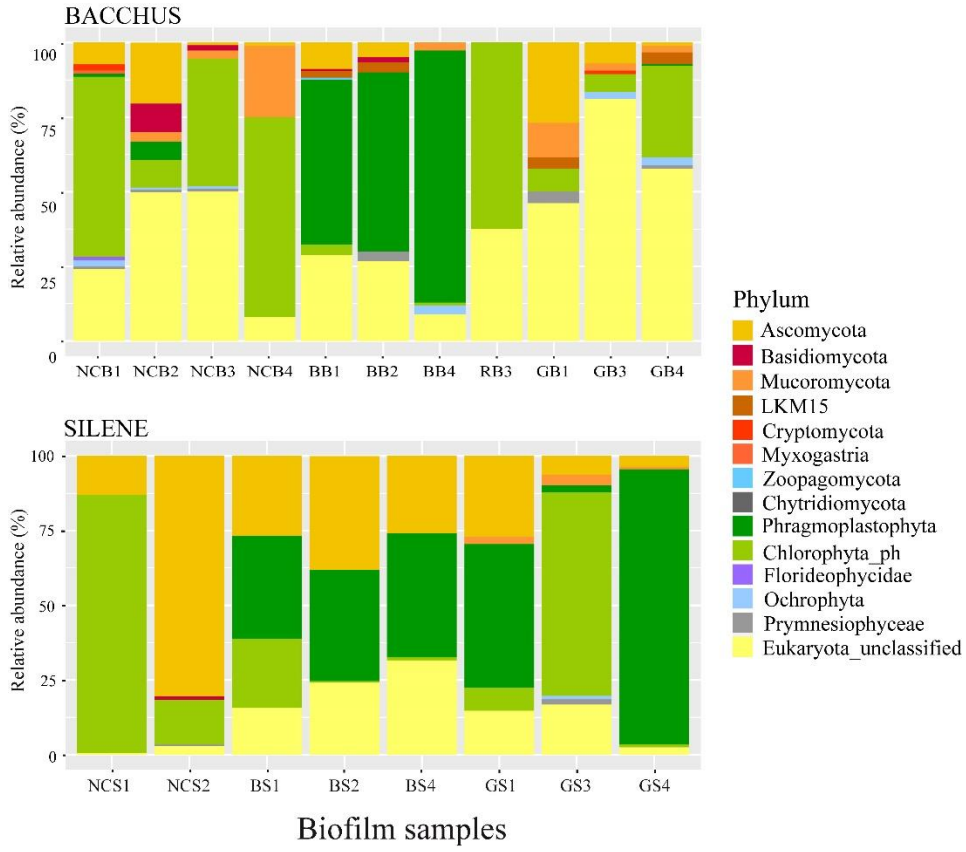

Fig. 4. Eukaryotic diversity at phylum level in Bacchus and Silene areas determined by Illumina based high-throughput sequencing. Only the phyla representing more than 0.5% of total sequences were considered.

3.7. Quantitative PCR

qPCR was carried out on 4 samples for each area except BB where only DNA could be extracted from only 2 samples and finally one sample gave results. In consequence, BB was excluded from the statistical analysis though its sole sample had the highest 16S and 18S rRNA gene copy numbers. Other samples had 16S and 18S gene copy numbers of 2.8-5.4x10^5 cp/ng and 1.3-2.1x10^5 cp/ng, respectively (Table 2). The 16S/18S ratio was remarkably similar for all areas with 2.6 (2.5 for GS).

Area	16S rRNA	18S rRNA	Ratio 16S/18S
NCB	$4.5.10^5 \pm 2.2.10^4$ ab	$1.7.10^5 \pm 8.2.10^3$ ab	$2.6 \pm 6.5.10^{-3}$ a
GB	$3.6.10^5 \pm 8.1.10^4$ ab	$1.4.10^5 \pm 3.0.10^4$ ab	$2.6 \pm 3.0.10^{-2}$ ab
BB	$6.0.10^5$	$2.3.10^5$	2.6
RB	$4.5.10^5 \pm 1.4.10^4$ ab	$1.7.10^5 \pm 5.3.10^4$ ab	$2.6 \pm 5.2.10^{-2}$ a
NCS	$5.4.10^5 \pm 1.5.10^4$ a	$2.1.10^5 \pm 5.5.10^4$ a	$2.6 \pm 3.7.10^{-3}$ a
GS	$2.8.10^5 \pm 1.6.10^4$ b	$1.3.10^5 \pm 7.3.10^4$ b	$2.5 \pm 8.2.10^{-2}$ b
BS	$5.0.10^5 \pm 9.6.10^4$ a	$1.9.10^5 \pm 3.5.10^4$ a	$2.6 \pm 2.4.10^{-2}$ a

Table 2. qPCR data with 16S rRNA and 18S rRNA (cp/ng DNAg) and the ratio 16S/18S. a, b correspond to statistically no-significant differences (Fisher's test, $p < 0.05$).

3.8. Identification of isolated microbial strains

The culture-based approach led to the isolation of 24 distinct bacterial strains whose partial 16S rRNA gene sequences were deposited into the NCBI Genbank database (Tables S5-S6). Thirteen and eleven strains were isolated and identified respectively from Bacchus and Silene. On both bas-reliefs, most strains belonged to the phylum Pseudomonadota with 9 bacterial strains in Bacchus and 7 in Silene. In

Bacchus, the area with the highest number of isolated bacterial strains was NCB with 5 strains comprising 3 Pseudomonadota affiliated to Alpha-Pseudomonadota (*Sphingopyxis macrogoltabida, Afipia massiliensis, Rhodospirillum sp.*) and 2 Actinomycetota (*Streptomyces cirratus* and *Saccharothrix sp.).* In RB, 3 Pseudomonadota were identified, one belonging to Alpha-Pseudomonadota and the genus *Mesorhizobium sp.* and two belonging to Gamma-Pseudomonadota and the species *Pseudomonas baetica* and *Acinetobacter radioresistens*. Four strains were identified in GB with 2 Alpha-Pseudomonadota (*Mesorhizobium sp.* and *Sphingopyxis sp*.), 1 Bacteroidota (*Pedobacter sp.*) and 1 Cyanobacteria (*Timaviella Dunensis*). Finally, only 1 Gamma-Pseudomonadota affiliated to *Lysobacter sp.* was isolated from BB. In Silene, BS was the area with the highest number of isolated bacterial strains (7), comprising 5 Pseudomonadota including 4 Alpha-Pseudomonadota (*Mesorhizobium sp.*, *Sphingopyxis alaskensis, Phyllobacterium sp.*, *Phyllobacterium trifolli* and 1 Gamma-Pseudomonadota (*Pseudomonas sp.*), 1 Actinomycetota (*Arthrobacter sp.*) and 1 Bacillota (*Paenibacillus sp.*). Then only 2 bacterial strains were sequenced in NCS with 1 Alpha-Pseudomonadota (*Aminobacter sp.*) and 1 Bacteroidota (*Dyadobacter sp.*) and in GS, 1 Alpha-Pseudomonadota (*Sphingopyxis sp*.) and 1 Bacteroidota (*Dyadobacter sp.*).

Twenty-five eukaryotic strains were isolated, including 15 fungal strains identified as Ascomycota with *Penicillium sp.* as main species present in every area and 10 phototrophs with Chlorophyta microalgae in most areas. In Bacchus, NCB had the highest number of fungi with 5 species all belonging to Ascomycota (*Aspergillus terreus, Cladosporium sp., Verticillium leptobactrum, Penicillium sp.*). The other areas had only 2 isolated strains like in GB with 1 Ascomycota (*Penicillium sp.*), 1 Basidiomycota (*Rhodotorula mucilaginosa*), in BB with 1 Ascomycota (*Penicillium limosum*), 1 Mucoromyceta (*Mortierella sp.*). Finally, in RB, only 1 strain classified as Ascomycota (*Penicillium brevicompactum*) was present. Eukaryotic phototrophs isolated in GB were 3 algae with *Diplosphaera sp.*, *Bracteacoccus sp.* and *Chromochloris zofingiensis.* In NCB, only *Diplosphaera sp.* was identified whereas in RB, only *Chromochloris zofingiensis* was sequenced. In Silene, from BS 3 fungi were identified with 2 Ascomycota (*Penicillium sp., Penicillium roqueforti*) and 1 Basidiomycota (*Sporidiobolus pararoseus*). In NCS, 1 Ascomycota as *Penicillium sp.* was also sequenced and 1 Basidiomycota (*Sporobolomyces ellipsoideus*). In GS, only 1 Ascomycota (*Penicillium sp.*) was also isolated. Finally, Chlorophyta microalgae with *Diplosphaera sp.* were identified in every area, then *Pseudostichococcus monallantoides* were sequenced in GS. The Bryophyta with *Eucladium verticillatum* was identified in BS.

3.9. Microscopic observations of phototrophs in biofilms

On Bacchus, in the NCB, a rod-like green morphotype similar to *Diplosphaera sp.* (Fig. S9), a green-blue filamentous morphotype similar to *Timaviella dunensis* and blue-green coccoid morphotype with 4 or 2 cells surrounded by a colourless mucilage which could associated to Cyanobacteria (Barberousse et al., 2006; Nugari et al., 2009) were observed. In GB, two green coccoid morphotypes similar to *Chromochloris zofingiensis* and bigger cells similar to *Bracteacoccus sp*. were observed, in addition to a green-blue coccoid morphotype with 4 or 2 cells in a colourless mucilage previously observed in NCB. In BB, the green-blue coccoid morphotype in NCB and GB also dominated but the cells were surrounded by an orange mucilage and the filamentous morphotype similar to *Timaviella dunensis* was secondarily observed. A coccoid green and yellow orange morphotype similar to *Chromochloris zofingiensis* algae and thick green filamentous morphotype were also described in this biofilm. RB was mainly composed of coccoid big red morphotype algae similar to *Chromochloris zofingiensis* and secondarily a green-blue tetra-shape morphotype as Cyanobacteria.

On Silene, a rod-like green morphotype similar to *Diplosphaera sp.* and a coccoid green morphotype were mostly observed in NCS. In GS, both previous morphotypes were observed together with a filamentous blue-green morphotype similar to *Timaviella dunensis*. Moreover, a new thick filamentous green morphotype, was noticed but not similar to any isolated strain. Finally, in BS, cells similar to *Diplosphaera sp.* and *Timaviella dunensis* were also observed, the green-blue coccoid morphotype with 4 or 2 cells surrounded by brownish mucilage and thick brown plant tissue-like filaments were very frequent and only observed in this area.

4. Discussion

This work investigated the lampenflora grown in two monumental bas-reliefs carved in the Pommery Champagne cellar, unique underground site as original chalk quarries transformed into a giant wine cellar in the 19th century. This subterranean environment with low variation of temperature, high relative humidity throughout the year and a water saturated stone, promotes the development of a lampenflora when the illumination of the bas-reliefs was settled for tourist visits. A strategy to control and prevent lampenflora needs to be found which includes a combination of several targets like the change of the environment management and the test of treatments to avoid the lampenflora growth for a longer time (Franco-Castillo et al., 2022). That firstly requires to characterise the different biofilm areas composing each artwork in the aim to define a relationship between them, and between the two artworks each located in the different pit. Measurements were carried out on first on the bas-reliefs by colourimetry, chlorophyll *a* fluorescence, pH measurements and sampling. That was completed by laboratory analyses of pigments, culture of microorganisms for genetic identification and high-throughput sequencing of 16S and 18S rRNA to determine the microbial diversity of the biofilms.

The molecular analyses carried out on 16S RNA firstly revealed that Bacchus had a higher bacterial richness than Silene. On Bacchus, GB and BB areas had the highest richness of OTUs while RB had the lowest. On Silene, GS had a lower diversity than NCS and BS. Bray-Curtis NMDS showed that the bacterial composition of the lampenflora of Bacchus was distinct from that of Silene. Moreover, it clearly clustered the samples from the different defined areas, more specifically in Bacchus where each area was characterized by a distinct bacterial diversity. Nonetheless, communities were mainly composed of Pseudomonadota in both bas-reliefs, mainly Alpha-Pseudomonadota, then Bacteroidota, Acidobacteriota and Actinomycetota. The dominance of those main plyla and especially Pseudomonadota was reported in show caves with illumination and, also karst caves in the darkness. Here proportions of Pseudomonadota were 45.5 % in Bacchus and 60 % in Silene, which was comparable to the lampenflora in French and Swiss show caves in which this phylum also dominated the bacterial community with 57.3 % (Pfendler et al., 2018b), and in Lehman caves in the USA with 35-70 % (Burgoyne et al., 2021). In karst caves, it also dominated in vermiculations with 41-54 % in Pertosa-Auletta Cave, southern Italy (Addesso et al., 2021).

Actinomycetota are often cited as a dominant phylum on par or with next to Pseudomonadota in show caves (20.2 %, 10-30% and 7-17 % in the last cited studies) but in the Pommery Cellar, they represented only 7 % for both bas-reliefs. Here, the ratio of Pseudomonadota to Actinomycetota was similar to vermiculations observed in alpine cave with between 36 to 46 % of Pseudomonadota and 4 to 11 % of Actinomycetota (Jurado et al., 2020). The dominance of Pseudomonadota in caves was already reported in communities exposed to high levels of human contact whereas natural cave bacterial community with low human contact was dominated by Firmicutes (Ikner et al., 2007). Here, Pseudomonadota were mostly represented by Alpha-Pseudomonadota and Gamma-Pseudomonadota among isolates, nonetheless the most abundant genera determined in the amplicon-sequencing were different than isolated microorganisms.

Those phyla are commonly identified outdoor in soils and on stone surface of monuments (Mihajlovski et al., 2017; Li et al., 2018; Romani et al., 2019), also in vermiculations thanks to the migration of bacteria from soils (Lavoie et al., 2017). The Pommery cellar was dug in highly fractured chalk promoting rainwater circulation and helping the migration of microorganisms from the upper surface. Pseudomonadota, Actinomycetota, Acidobacteriota are commonly described in karst caves (Burgoyne et al., 2021; Ai et al., 2022) and in catacombs often with a dominance of Pseudomonadota or Actinomycetota (Saarela et al., 2004; Urzì et al., 2010).

The comparison of the taxonomic diversity showed that Bacchus had a higher abundance of secondary phyla than Silene with Chlamydiota, Chloroflexota, Gemmatimonadota. In Bacchus, samples from each area were composed of a similar community at the genus level except for GB in which the three samples had distinct communities. NCB could be characterized by a high abundance of *Dongia* and *Rhizobiales* (*Hyphomicrobium, Rhizobiales Incertae sedis)*, BB by *Microscillaceae* unclassified and RB by *Hirschia* which are bacteria from soil and water (Hahnke et al., 2016; Kim et al., 2016). In Silene, NCS

samples had a relative similar community with a dominance of *Rhizobiaceae* and *Hyphomicrobium* (both from *Rhizobiales* order) as bacteria from soil origin. *Rhizobiaceae*, which were the most abundant Pseudomonadota in the amplicon sequencing and were also sequenced in culture with *Mesorhizobium sp.* in RB, GB and BS, are nitrogen-fixing species (Addesso et al., 2021) and reported as responsible to the deterioration of tomb (Diaz-Herraiz et al., 2014), and *Hyphomicrobium g.* can correspond to iron and manganese-oxidizing bacteria involved in Mn precipitation (Northup et al., 2003; Miller et al., 2020).

Cyanobacteria, phototrophic bacteria whose metabolic activity produces carbonic acid and dissolves limestone, were weakly abundant in every area of both bas-reliefs (up to 5.5 % in GS) which suggested that the green colour of GB, BB and GS was weakly associated with them. This result was surprising since Cyanobacteria are considered the pioneering inhabitants in the colonisation of caves (Czerwik-Marcinkowska and Mrozińska, 2011) and the main taxa with 72 % of the phototrophic microbiota in hypogean habitats (Popkova et al., 2019) and up to 100 % when no Chlorophyta were detected (S. Pfendler et al., 2018b). Chroococcales and Nostocales represented here by *Chalicogloea cavernicola* (up to 1.3 % in GB), could correspond to the observed coccoid blue green morphotype in NCB, GB and BB. Those phyla were often recorded as main cyanobacteria with respectively for the both 40.7 % and 51.2 % (Pfendler et al., 2018b). *Leptolyngbya* was the genus mainly sequenced in GS but also present in BB on Bacchus and in NCS and BS on Silene. This phylum was dominated cyanobacteria in hypogea (Bruno et al., 2009). Here, it could be associated to *Timaviella Dunensis* isolated from BS. Those species were recently described from sand dunes (Mikhailyuk et al., 2022), other species, *Timaviella* Sciuto & Moro, as recent cryptic genus created from the separation of the morphologically close *Leptolyngbya*, were from underground environment similar to Pommery cellar environment but species determined by Sciuto & Moro corresponded to red-brownish morphotype (Sciuto et al., 2017).

The eukaryotic 18S rRNA sequencing displayed a weak content of OTUs which did not reflect the real microbial richness of the areas specially for phototrophic microorganisms abundantly observed in microscopy. Nonetheless, the relative abundance showed the net higher proportion of phototrophs than organoheterotrophs. Moreover, it revealed the same results than in 16S rRNA analysis, that meant distinct microbial communities in Bacchus and Silene. Bacchus displayed a weaker content of fungi than Silene. Ascomycota were dominant especially in Silene with *Hypocreales* unclassified, Chaetothyriales unclassified, *Plectosphaerella* and *Fusarium*; whereas in Bacchus, Ascomycota were most represented by *Calcarisporiella* and Mucoromycota by *Mortierella*. They were the most frequently sequenced phylum from cultured species with *Penicillium sp*. and were found in show caves with 71.3 % (Pfendler et al., 2018b) and a cave church 73.8 % (Ljaljević Grbić et al., 2022) and in above-ground heritage sites (Mascaro et al., 2021). Furthermore, despite a high proportion of eukaryote unclassified in the sequencing of samples, each area of Bacchus (except GB) had a distinct eukaryotic community with a dominance of phototrophs: NCB was characterized by *Chromochloris* (except NCB2), BB by Embryophyta unclassified, RB by *Chromochloris*. Only GB samples displayed a heterogeneous community in samples with the dominance of fungi (*Chitinophagaceae* unclassified - GB1) or *Chromochloris* (GB4). In Silene, more dissimilarities in the community were showed within areas, NCS was dominated by the algae *Stichococcus* or the fungus *Plectosphaerella*. Nonetheless, GS and BS were dominated by Embryophyta unclassified (except GS3) like *Eucladium verticillatum* which were cultured from BS.

Notably, *Chromochloris* algae were specially developed in Bacchus whereas *Stichococcus* specially grew in Silene. The environmental conditions of both bas-reliefs were similar, comprising temperature, relative humidity and the high content of water in chalk on which lampenflora developed, only the lighting conditions varied over time which could explain the variation of the composition of the microbial communities located in the two different pits of the same cellar. *Diplosphaera sp.* and *Pseudostichococcus sp.* sequenced from isolated strains from both Bacchus and Silene, belong to *Stichococcus* genus and are widely in many environments (freshwaters, marine and terrestrial ecosystems and in harsh polar environments (Proeschold and Darienko, 2020; Chiva et al., 2022).

The genus *Chromochloris* was the main phototrophs in RB and belongs to the Chlorophyta or green algae, although the taxonomy has been revisited several times (Fucikova and Lewis, 2012). Cells showed, however, marked red pigmentation in this area. Strains have been cultivated from RB and identified as *Chromochloris zofingiensis*, also showing red morphotype, whereas isolates from GB were green. Moreover, *C. zofingiensis* cultivated in laboratory in Hoagland liquid medium always showed green morphotype whereas the showed red-orange colour when grown on the surface of chalk stone at the natural daylight for many months. This genus was often studied and selected for the abilities to produce a high content of carotenoids for potential applications in pharmaceutical industries, and more specifically secondary carotenoids as astaxanthin accumulated in lipid bodies outside the chloroplast (Liu et al., 2014). The accumulation of astaxanthin was associated with stress conditions (high light, nitrogen starvation, high salinity) to protect algal cells against oxidative damage (Liu et al., 2014; Maltsev et al., 2021) and in a mixotrophic medium with glucose content (Azaman et al., 2017; Sun et al., 2019), which were on the opposite of the natural and drastic cellar conditions. Nonetheless, an accumulation of astaxanthin was already performed in laboratory under limited light condition and nitrogen depletion (Mulders et al., 2015) and it was also associated to mature cells from cultures more than 4 months old (Fucikova and Lewis, 2012).

The results of qPCR revealed that bacterial 16S rRNA gene copy numbers 2.6 times as high as 18S, with remarkably constant ratio values, suggesting equal proportions of bacteria and fungi or other eucaryotes in all samples. Fisher test noticed that there was no statistical difference of 16S rRNA and 18S rRNA of every area on Bacchus and only GS was significantly different from the others. However, the number of genes encoding for 16S/18S rRNA can vary among the microorganisms (Větrovský and Baldrian, 2013; Gong and Marchetti, 2019) and this variability may influence the diversity and abundance of the species determined in the different samples. One limit of the qPCR approach we followed is that it is, as such, unable to investigate differences in the extent of biological colonization. To this end, biofilm sampling from precisely measured areas and recording of the collected mass, followed by DNA extraction and dosing as well as qPCR analysis, would be necessary to estimate the biomass per surface unit and will be included in future studies. Furthermore, all extracted DNA does not necessarily correspond to living cells, extracellular DNA being present in the biofilms after cell death.

The alkaline pH observed for all Bacchus areas was in agreement with the dominance of the limestone in this area. The non-coloured NCB area was the most alkaline with pH = 8.6 whereas pH in the coloured areas BB and RB was slightly lower and the lowest for GB, which suggested its microbial community could decrease the alkalinity with the production of extracellular compounds (enzymes, acids) by bacteria and fungi (Warscheid and Braams, 2000; Saarela et al., 2004; Stanaszek-Tomal, 2020). All Silene areas had a neutral pH. This result was probably due to distinct communities on each artwork and to the dominance of bacteria most of which prefer an inert or slightly alkaline pH (Stanaszek-Tomal, 2020).

Analysis of pigments in the Bacchus areas showed a low chl. *a* content for NCB, it was higher in GB and much higher in BB which coincided with the progressive greening showing by a^* of those areas. BB had the highest values of chl. *a* and *b* pigments and carotenoids which could explain the dark green colour measured in colourimetry. The high content of carotenoids in RB confirmed the high potential of *Chromochloris* to provide this pigment probably when a light intensity was much higher in the Bacchus pit and presently because of a low nutriment substrate and a growth over a very long period. Moreover, those algae were probably not the only source of carotenoids since the 16S rRNA sequencing indicated RB had 18.5 % of the carotenoid-producing Xanthomonadales reads (Chen et al., 2009; Porca et al., 2012; Addesso et al., 2021) and 13 to 27 % of *Hirschia* reads (Bontemps et al., 2023). Concentrations of carotenoids were low in NCB and GB, suggesting that the cells of *Chromochloris*, the most abundant algal genus present in 18S rRNA dataset, were green and that the biofilm was at an earlier development stage than in RB, given the expansion of this biofilm from the middle to the periphery of the artwork and maybe because of a competition with other microorganisms. In addition,

the presence of Rhizobiales (21 and 31 % respectively in NCB and GB) provide nitrogen to algae leading to limit stress conditions. RB area displayed a high content of the three phycobiliproteins which was not in accordance with Cyanobacteria 16S rRNA analysis since the abundance was very weak. PBPs, common pigments in Cyanobacteria, can also be produced by algae like Rhodophyta and Cryptophyta (Maltsev et al., 2021) but such algae were not detected here. Consequently, 16S rRNA analysis could under-estimated the abundance of Cyanobacteria in the lampenflora areas of Bacchus. Moreover, the photosynthetic activity of RB measured through the effective quantum yield of the photosystem II (ϕ_{PSII}) from the chl. *a* pigment in Chlorophyta, was higher than in green areas (GB and BB) despite the lowest chl. *a* concentration which could limit the photosynthetic activity but the high content of PBPs in RB promoted the absorption of excitation energy by phycobilisomes and transferred to the chlorophyll molecules in the PSII and ascertained the presence of Cyanobacteria (Grossman et al., 1994).

In Silene, GS had a high PBP content, the Cyanobacteria abundance was the highest compared with the other areas, but it remained low (5.5 %). Besides, this area displayed the highest concentrations of chlorophyll pigments probably associated to Embryophyta and *Stichococcus*. The high PBP content in RB and GS highlighted the ability of Cyanobacteria to adapt to various wavelengths of the electromagnetic spectrum that chlorophyll pigments and carotenoids cannot absorb (Albertano et al., 2003; Korbee et al., 2005; Muñoz-Fernández et al., 2021) and to an intensity which is currently weak (0.1 µmol photons.m^{-2}.s^{-1}) that suggested those species can survive at a photon flux lower than their photosynthetic compensation point (Mulec and Kosi, 2009; D'Agostino et al., 2015).

The lack of information concerning the history of cellar outfitting (including lighting), bas-relief cleaning and repairing does not allow to establish a precise chronology of biofilm development. The tourist attractiveness of the cellar required to improve the lighting to secure the premises and to highlight the monumental artworks. The frequent air flow and people from outside provide an easy seeding and spreading of opportunistic microorganisms which coat mineral surfaces and deteriorate them over time. Controlling the air flow seems complicated due to the activities of the wine cellar but the artificial illumination specifically on monumental bas-reliefs could be more adapted to avoid the lampenflora growth. Efforts have already been carried out to illuminate bas-reliefs with for a reduced time. Cyanobacteria and algae are, however, able to survive and develop in low lighting conditions (Baquedano Estévez et al., 2019) and the constant lighting of modern artworks laid on the ground, though low, is sufficient for their growth. Moving the temporary artworks to other pits would deprive the lampenflora of this growth energy. Finally, the design of a lighting including lamps with a spectral light emission of less photosynthetic effectiveness, such as green light less absorbed by chlorophylls and carotenoids, could also be beneficial (Sanmartín et al., 2017). On the opposite, red-orange and blue lights are the most effective for the algal proliferation (Cigna and Forti, 2013), but cyanobacteria are well-known to develop in humid and dimly lit environments and are able to adjust the content of phycobiliproteins in response to a short shift on the light quality (Maltsev et al., 2021). Nonetheless, the best results to limit the photosynthetic growth were achieved with a 'testing light' corresponding to an emission between 420-470 nm and between 500-670 nm (Bruno and Valle, 2017).

5. Conclusion

Lampenflora growing on bas-reliefs is mainly exogenous and opportunistic. Contrary to our hypothesis, both phototrophic and non-phototrophic microorganisms differ in diversity and abundance between bas-reliefs and between areas defined within the bas-reliefs, in spite of a remarkably constant bacteria-to-fungi ratio. Bacchus, with *Chromochloris* algae as the main phototrophs, had a higher microbial diversity than Silene, on which Embryophyta and *Stichococcus* were dominant. Areas defined visually from the biofilm colour matched a specific community in Bacchus, which was not the case for Silene. The strategy to control the lampenflora growth on the bas-reliefs should raise a sustainable preservation program including the preservation of bas-reliefs and the tourist visits by refine the heritage management on two sides: an adaptation of the environment with a new tourist path in moving the contemporary artworks in pits without bas-reliefs and by changing of the lighting system by the selection of wavelengths less favourable for the photosynthetic growth. The second side

intervenes on the bas-reliefs by the application of a preventive chemical treatment to delay the recolonization or the installation of UV-C lamps that would work at night in absence of visitors.

Acknowledgements

The study was supported and funded by Vranken-Pommery group.

References

Addesso, R., Gonzalez-Pimentel, J.L., D'Angeli, I.M., De Waele, J., Saiz-Jimenez, C., Jurado, V., Miller, A.Z., Cubero, B., Vigliotta, G., Baldantoni, D., 2021. Microbial Community Characterizing Vermiculations from Karst Caves and Its Role in Their Formation. Microb Ecol 81, 884–896. https://doi.org/10.1007/s00248-020-01623-5

Ai, J., Guo, J., Li, Y., Zhong, X., Lv, Y., Li, J., Yang, A., 2022. The diversity of microbes and prediction of their functions in karst caves under the influence of human tourism activities—a case study of Zhijin Cave in Southwest China. Environ Sci Pollut Res 29, 25858–25868. https://doi.org/10.1007/s11356-021-17783-x

Albertano, P., Moscone, D., Palleschi, G., Hermosin, B., Saiz-Jimenez, C., Sanchez-Moral, S., Hernández-Mariné, M., Urzi, C., Groth, I., Schroeckh, V., 2003. Cyanobacteria attack rocks (CATS): control and preventive strategies to avoid damage caused by cyanobacteria and associated microorganisms in Roman hypogean monuments. Molecular biology and cultural heritage 151–162.

Ariño, X., Llop, E., Gómez-Bolea, A., Saiz-Jimenez, C., 2010. Effects of climatic change on microorganisms colonizing cultural heritage stone materials. Climate change and cultural heritage 193–198.

Azaman, S.N.A., Nagao, N., Yusoff, F.M., Tan, S.W., Yeap, S.K., 2017. A comparison of the morphological and biochemical characteristics of Chlorella sorokiniana and Chlorella zofingiensis cultured under photoautotrophic and mixotrophic conditions. PeerJ 5, e3473. https://doi.org/10.7717/peerj.3473

Baquedano Estévez, C., Merino, L.M., Almudena de la Losa, R., Valsero, J.D., 2019. The lampenflora in show caves and its treatment: an emerging ecological problem. International Journal of Speleology 48. https://doi.org/10.5038/1827-806X.48.3.2263

Barberousse, H., Tell, G., Yéprémian, C., Couté, A., 2006. Diversity of algae and cyanobacteria growing on building façades in France. Algological Studies 120, 81–105. https://doi.org/10.1127/1864-1318/2006/0120-0081

Bastian, F., Alabouvette, C., 2009. Lights and shadows on the conservation of a rock art cave: the case of Lascaux Cave. International Journal of Speleology 38, 55–60. https://doi.org/10.1007/s00114-009-0540-y

Bennett, A., Bogorad, L., 1973. Complementary chromatic adaptation in a filamentous blue-green alga. J Cell Biol 58, 419–435. https://doi.org/10.1083/jcb.58.2.419

Bontemps, Z., Prigent-Combaret, C., Guillmot, A., Hugoni, M., Moënne-Loccoz, Y., 2023. Dark-zone alterations expand throughout Paleolithic Lascaux Cave despite spatial heterogeneity of the cave microbiome. Environmental Microbiome 18, 31. https://doi.org/10.1186/s40793-023-00488-8

Bruno, L., Billi, D., Bellezza, S., Albertano, P., 2009. Cytomorphological and Genetic Characterization of Troglobitic Leptolyngbya Strains Isolated from Roman Hypogea. Applied and Environmental Microbiology 75, 608–617. https://doi.org/10.1128/AEM.01183-08

Bruno, L., Rugnini, L., Spizzichino, V., Caneve, L., Canini, A., Ellwood, N.T.W., 2019. Biodeterioration of Roman hypogea: the case study of the Catacombs of SS. Marcellino and Pietro (Rome, Italy). Annals of Microbiology 69, 1023–1032. https://doi.org/10.1007/s13213-019-01460-z

Bruno, L., Valle, V., 2017. Effect of white and monochromatic lights on cyanobacteria and biofilms from Roman Catacombs. International Biodeterioration & Biodegradation 123, 286–295. https://doi.org/10.1016/j.ibiod.2017.07.013

Burgoyne, J., Crepeau, R., Jensen, J., Smith, H., Baker, G., Leavitt, S.D., 2021. Lampenflora in a Show Cave in the Great Basin Is Distinct from Communities on Naturally Lit Rock Surfaces in Nearby Wild Caves. Microorganisms 9, 1188. https://doi.org/10.3390/microorganisms9061188

Cennamo, P., Montuori, N., Trojsi, G., Fatigati, G., Moretti, A., 2016. Biofilms in churches built in grottoes. Science of The Total Environment 543, 727–738. https://doi.org/10.1016/j.scitotenv.2015.11.048

Chen, Y., Wu, L., Boden, R., Hillebrand, A., Kumaresan, D., Moussard, H., Baciu, M., Lu, Y., Colin Murrell, J., 2009. Life without light: microbial diversity and evidence of sulfur- and ammonium-based chemolithotrophy in Movile Cave. ISME J 3, 1093–1104. https://doi.org/10.1038/ismej.2009.57

Chiva, S., Moya, P., Barreno, E., 2022. Lichen phycobiomes as source of biodiversity for microalgae of the Stichococcus-like genera. Biologia. https://doi.org/10.1007/s11756-022-01223-3

Cigna, A.A., Forti, P., 2013. Caves: the most important geotouristic feature in the world. Tourism and Karst areas 6, 9–26.

Comeau, A.M., Li, W.K.W., Tremblay, J.-É., Carmack, E.C., Lovejoy, C., 2011. Arctic Ocean Microbial Community Structure before and after the 2007 Record Sea Ice Minimum. PLOS ONE 6, e27492. https://doi.org/10.1371/journal.pone.0027492

Czerwik-Marcinkowska, J., Mrozińska, T., 2011. Algae and cyanobacteria in caves of the Polish Jura. Polish Botanical Journal 56, 203–243.

D'Agostino, D., Beccarisi, L., Camassa, M., Febbroriello, P., 2015. Microclimate and microbial characterization in the Zinzulusa show cave (South Italy) after switching to led lighting. Journal of Cave and Karst Studies 77, 133–144. https://doi.org/10.4311/2014EX0123

Del Rosal, Y., Muñoz-Fernández, J., Celis-Plá, P., Hernández-Mariné, M., Álvarez-Gómez, F., Merino, S., Figueroa, F., 2021. Monitoring photosynthetic activity using in vivo chlorophyll a fluorescence in microalgae and cyanobacteria biofilms in the Nerja Cave (Malaga, Spain). International Journal of Speleology 51. https://doi.org/10.5038/1827-806X.51.1.2404

Diaz-Herraiz, M., Jurado, V., Cuezva, S., Laiz, L., Pallecchi, P., Tiano, P., Sanchez-Moral, S., Saiz-Jimenez, C., 2014. Deterioration of an Etruscan tomb by bacteria from the order Rhizobiales. Sci Rep 4, 3610. https://doi.org/10.1038/srep03610

Duan, Y., Wu, F., He, D., Gu, J.-D., Feng, H., Chen, T., Liu, G., Wang, W., 2021. Bacterial and fungal communities in the sandstone biofilms of two famous Buddhist grottoes in China. International Biodeterioration & Biodegradation 163, 105267. https://doi.org/10.1016/j.ibiod.2021.105267

European committee for Standardization, 2011. CSN EN ISO 11664-4 - Colorimetry - Part 4: CIE 1976 L*a*b* Colour space (ISO 11664- 4:2008), Category: 0117 Optics. https://www.iso.org/standard/74166.html

Eyssautier-Chuine, S., Vaillant-Gaveau, N., Charpentier, E., Reffuveille, F., 2021. Comparison of biofilm development on three building and restoration stones used in French monuments. International Biodeterioration & Biodegradation 165, 105322. https://doi.org/105322. 10.1016/j.ibiod.2021.105322

Ezraty, B., Henry, C., Hérisse, M., Denamur, E., Barras, F., 2014. Commercial Lysogeny Broth culture media and oxidative stress: A cautious tale. Free Radical Biology and Medicine 74, 245–251. https://doi.org/10.1016/j.freeradbiomed.2014.07.010

Franco-Castillo, I., Misra, A., Laratte, S., Gommeaux, M., Perarnau, R., Vaillant-Gaveau, N., Pierlot, C., Streb, C., Mitchell, S.G., Eyssautier-Chuine, S., 2022. New protective coatings against lampenflora growing in the Pommery Champagne cellar. International Biodeterioration & Biodegradation 173, 105459. https://doi.org/10.1016/j.ibiod.2022.105459

Fucikova, K., Lewis, L.A., 2012. Intersection of Chlorella, Muriella and Bracteacoccus: resurrecting the genus Chromochloris kol et chodat (Chlorophyceae, Chlorophyta). Fottea 12, 83–93. https://doi.org/10.5507/fot.2012.007

902 Gong, W., Marchetti, A., 2019. Estimation of 18S Gene Copy Number in Marine Eukaryotic Plankton
903 Using a Next-Generation Sequencing Approach. Frontiers in Marine Science 6.
904 https://doi.org/10.3389/fmars.2019.00219
905 Grossman, A.R., Schaefer, M.R., Chiang, G.G., Collier, J.L., 1994. The Responses of Cyanobacteria to
906 Environmental Conditions: Light and Nutrients, in: Bryant, D.A. (Ed.), The Molecular Biology
907 of Cyanobacteria, Advances in Photosynthesis. Springer Netherlands, Dordrecht, pp. 641–
908 675. https://doi.org/10.1007/978-94-011-0227-8_21
909 Hahnke, R.L., Meier-Kolthoff, J.P., García-López, M., Mukherjee, S., Huntemann, M., Ivanova, N.N.,
910 Woyke, T., Kyrpides, N.C., Klenk, H.-P., Göker, M., 2016. Genome-Based Taxonomic
911 Classification of Bacteroidetes. Frontiers in Microbiology 7.
912 https://doi.org/10.3389/fmicb.2016.02003
913 Ikner, L.A., Toomey, R.S., Nolan, G., Neilson, J.W., Pryor, B.M., Maier, R.M., 2007. Culturable
914 Microbial Diversity and the Impact of Tourism in Kartchner Caverns, Arizona. Microb Ecol 53,
915 30–42. https://doi.org/10.1007/s00248-006-9135-8
916 Jurado, V., Gonzalez-Pimentel, J.L., Miller, A.Z., Hermosin, B., D'Angeli, I.M., Tognini, P., De Waele, J.,
917 Saiz-Jimenez, C., 2020. Microbial Communities in Vermiculation Deposits from an Alpine
918 Cave. Frontiers in Earth Science 8. https://doi.org/10.3390/app10103448
919 Kim, D.-U., Lee, H., Kim, H., Kim, S.-G., Ka, J.-O., 2016. Dongia soli sp. nov., isolated from soil from
920 Dokdo, Korea. Antonie Van Leeuwenhoek 109, 1397–1402. https://doi.org/10.1007/s10482-
921 016-0738-x
922 Korbee, N., Figueroa, F.L., Aguilera, J., 2005. Effect of light quality on the accumulation of
923 photosynthetic pigments, proteins and mycosporine-like amino acids in the red alga
924 Porphyra leucosticta (Bangiales, Rhodophyta). Journal of Photochemistry and Photobiology
925 B: Biology 80, 71–78. https://doi.org/10.1016/j.jphotobiol.2005.03.002
926 Lavoie, K.H., Winter, A.S., Read, K.J.H., Hughes, E.M., Spilde, M.N., Northup, D.E., 2017. Comparison
927 of bacterial communities from lava cave microbial mats to overlying surface soils from Lava
928 Beds National Monument, USA. PLOS ONE 12, e0169339.
929 https://doi.org/10.1371/journal.pone.0169339
930 Li, Q., Zhang, B., Yang, X., Ge, Q., 2018. Deterioration-associated microbiome of stone monuments:
931 structure, variation, and assembly. Applied and environmental microbiology 84.
932 https://doi.org/10.1128/AEM.02680-17
933 Lienhard, P., Tivet, F., Chabanne, A., Dequiedt, S., Lelièvre, M., Sayphoummie, S., Leudphanane, B.,
934 Prévost-Bouré, N.C., Séguy, L., Maron, P.-A., Ranjard, L., 2013. No-till and cover crops shift
935 soil microbial abundance and diversity in Laos tropical grasslands. Agron. Sustain. Dev. 33,
936 375–384. https://doi.org/10.1007/s13593-012-0099-4
937 Liu, J., Sun, Z., Gerken, H., Liu, Z., Jiang, Y., Chen, F., 2014. Chlorella zofingiensis as an Alternative
938 Microalgal Producer of Astaxanthin: Biology and Industrial Potential. Marine Drugs 12, 3487–
939 3515. https://doi.org/10.3390/md12063487
940 Ljaljević Grbić, M., Dimkić, I., Savković, Ž., Stupar, M., Knežević, A., Jelikić, A., Unković, N., 2022.
941 Mycobiome Diversity of the Cave Church of Sts. Peter and Paul in Serbia—Risk Assessment
942 Implication for the Conservation of Rare Cavern Habitat Housing a Peculiar Fresco Painting.
943 Journal of Fungi 8, 1263. https://doi.org/10.3390/jof8121263
944 Maltsev, Y., Maltseva, K., Kulikovskiy, M., Maltseva, S., 2021. Influence of Light Conditions on
945 Microalgae Growth and Content of Lipids, Carotenoids, and Fatty Acid Composition. Biology
946 10, 1060. https://doi.org/10.3390/biology10101060
947 Martin-Sanchez, P.M., Jurado, V., Porca, E., Bastian, F., Lacanette, D., Alabouvette, C., Saiz-Jimenez,
948 C., 2014. Airborne microorganisms in Lascaux cave (France). International Journal of
949 Speleology, Tampa, FL (USA) 43, 295–303. https://doi.org/10.5038/1827-806X.43.3.6
950 Mascaro, M.E., Pellegrino, G., Palermo, A.M., 2021. Analysis of biodeteriogens on architectural
951 heritage. An approach of applied botany on a gothic building in southern Italy. Sustainability
952 14, 34. https://doi.org/10.3390/su14010034

Mihajlovski, A., Gabarre, A., Seyer, D., Bousta, F., Di Martino, P., 2017. Bacterial diversity on rock surface of the ruined part of a French historic monument: The Chaalis abbey. International Biodeterioration & Biodegradation 120, 161–169. https://doi.org/10.1016/j.ibiod.2017.02.019

Mikhailyuk, T., Vinogradova, O., Holzinger, A., Glaser, K., Akimov, Y., Karsten, U., 2022. Timaviella dunensis sp. nov. from sand dunes of the Baltic Sea, Germany, and emendation of Timaviella edaphica (Elenkin) O.M. Vynogr. & Mikhailyuk (Synechococcales, Cyanobacteria) based on an integrative approach. Phytotaxa 532, 192–208. https://doi.org/10.11646/phytotaxa.532.3.1

Miller, A.Z., García-Sánchez, A.M., L. Coutinho, M., Costa Pereira, M.F., Gázquez, F., Calaforra, J.M., Forti, P., Martínez-Frías, J., Toulkeridis, T., Caldeira, A.T., Saiz-Jimenez, C., 2020. Colored Microbial Coatings in Show Caves from the Galapagos Islands (Ecuador): First Microbiological Approach. Coatings 10, 1134. https://doi.org/10.3390/coatings10111134

Miller, A.Z., Rogerio Candelera, M.A., Dionísio, A., Macedo, M.F., Saiz-Jimenez, C., 2011. Microalgae as biodeteriogens of stone cultural heritage: qualitative and quantitative research by non-contact techniques. (IRNAS) Libros y partes de libros 345–358.

Mulders, K.J.M., Weesepoel, Y., Bodenes, P., Lamers, P.P., Vincken, J.-P., Martens, D.E., Gruppen, H., Wijffels, R.H., 2015. Nitrogen-depleted Chlorella zofingiensis produces astaxanthin, ketolutein and their fatty acid esters: a carotenoid metabolism study. J Appl Phycol 27, 125–140. https://doi.org/10.1007/s10811-014-0333-3

Mulec, J., Kosi, G., 2009. Lampenflora algae and methods of growth control. Journal of cave and karst studies, A Publication of the National Speleological Society 71, 109–115.

Mulec, J., Kosi, G., Vrhovšek, D., 2008. Characterization of cave aerophytic algal communities and effects of irradiance levels on production of pigments. Journal of Cave and Karst Studies 70, 3–12.

Mulec, J., Vaupotič, J., Walochnik, J., 2012. Prokaryotic and Eukaryotic Airborne Microorganisms as Tracers of Microclimatic Changes in the Underground (Postojna Cave, Slovenia). Microb Ecol 64, 654–667. https://doi.org/10.1007/s00248-012-0059-1

Muñoz-Fernández, J., Del Rosal, Y., Álvarez-Gómez, F., Hernández-Mariné, M., Guzmán-Sepúlveda, R., Korbee, N., Figueroa, F.L., 2021. Selection of LED lighting systems for the reduction of the biodeterioration of speleothems induced by photosynthetic biofilms in the Nerja Cave (Malaga, Spain). Journal of Photochemistry and Photobiology B: Biology 217, 1–10. https://doi.org/10.1016/j.jphotobiol.2021.112155

Northup, D.E., Barns, S.M., Yu, L.E., Spilde, M.N., Schelble, R.T., Dano, K.E., Crossey, L.J., Connolly, C.A., Boston, P.J., Natvig, D.O., Dahm, C.N., 2003. Diverse microbial communities inhabiting ferromanganese deposits in Lechuguilla and Spider Caves. Environmental Microbiology 5, 1071–1086. https://doi.org/10.1046/j.1462-2920.2003.00500.x

Nugari, M.P., Pietrini, A.M., Caneva, G., Imperi, F., Visca, P., 2009. Biodeterioration of mural paintings in a rocky habitat: The Crypt of the Original Sin (Matera, Italy). International Biodeterioration & Biodegradation 63, 705–711. https://doi.org/10.1016/j.ibiod.2009.03.013

Oren, A., Garrity, G.M., 2021. Valid publication of the names of forty-two phyla of prokaryotes. International Journal of Systematic and Evolutionary Microbiology 71, 005056. https://doi.org/10.1099/ijsem.0.005056

Perez, R.E., 2018. Study and remediation of environmental problems caused due to the growth of algae in speleothems of calcareous caves adapted for tourism- a case of success in Spain. J Environ Geol 02, 20–27. https://doi.org/10.4172/2591-7641.1000013

Pfendler, S., Borderie, F., Bousta, F., Alaoui-Sossé, L., Alaoui-Sossé, B., Aleya, L., 2018a. Comparison of biocides, allelopathic substances and UV-C as treatments for biofilm proliferation on heritage monuments. Journal of Cultural Heritage 33, 117–124. https://doi.org/10.1016/j.culher.2018.03.016

Pfendler, S., Karimi, B., Maron, P.-A., Ciadamidaro, L., Valot, B., Bousta, F., Alaoui-Sosse, L., Alaoui-Sosse, B., Aleya, L., 2018b. Biofilm biodiversity in French and Swiss show caves using the

metabarcoding approach: First data. Science of the Total Environment 615, 1207–1217. https://doi.org/10.1016/j.scitotenv.2017.10.054
Popkova, A., Mazina, S., Lashenova, T., 2019. Phototrophic communities of Ahshtyrskaya Cave in the condition of artificial light. Ecologica Montenegrina 23, 8–19.
Porca, E., Jurado, V., Žgur-Bertok, D., Saiz-Jimenez, C., Pašić, L., 2012. Comparative analysis of yellow microbial communities growing on the walls of geographically distinct caves indicates a common core of microorganisms involved in their formation. FEMS Microbiology Ecology 81, 255–266. https://doi.org/10.1111/j.1574-6941.2012.01383.x
Proeschold, T., Darienko, T., 2020. The green puzzle Stichococcus (Trebouxiophyceae, Chlorophyta): New generic and species concept among this widely distributed genus. Phytotaxa 441, 113–142. https://doi.org/10.11646/phytotaxa.441.2.2
R Core Team, 2023. R: A Language and Environment for Statistical Computing-R Foundation for Statistical Computing. http://www.R-project. org/
Romani, M., Carrion, C., Fernandez, F., Intertaglia, L., Pecqueur, D., Lebaron, P., Lami, R., 2019. High bacterial diversity in pioneer biofilms colonizing ceramic roof tiles. International Biodeterioration & Biodegradation 144, 104745. https://doi.org/10.1016/j.ibiod.2019.104745
Saarela, M., Alakomi, H.-L., Suihko, M.-L., Maunuksela, L., Raaska, L., Mattila-Sandholm, T., 2004. Heterotrophic microorganisms in air and biofilm samples from Roman catacombs, with special emphasis on actinobacteria and fungi. International biodeterioration & biodegradation 54, 27–37. https://doi.org/10.1016/j.ibiod.2003.12.003
Saiz-Jimenez, C., Cuezva, S., Jurado, V., Fernandez-Cortes, A., Porca, E., Benavente, D., Cañaveras, J.C., Sanchez-Moral, S., 2011. Paleolithic art in peril: policy and science collide at Altamira Cave. Science 334, 42–43. https://doi.org/10.1126/science.1206788
Salamah, A., Fadilah, N., Khoiriyah, I., Hendrayanti, D., 2019. Application of N2-Fixing Cyanobacteria Nostoc sp. SO-A31 to Hydroponically Grown Water Spinach (Ipomoea aquatic L.). AGRIVITA, Journal of Agricultural Science 41, 325–334. https://doi.org/10.17503/agrivita.v41i2.1867
Sanmartín, P., Vázquez-Nion, D., Arines, J., Cabo-Domínguez, L., Prieto, B., 2017. Controlling growth and colour of phototrophs by using simple and inexpensive coloured lighting: A preliminary study in the Light4Heritage project towards future strategies for outdoor illumination. International Biodeterioration & Biodegradation 122, 107–115. https://doi.org/10.1016/j.ibiod.2017.05.003
Sarkar, A., Rousseau, J., Hartmann-Thompson, C., Maples, C., Parker, J., Joyce, P., Scheide, J.I., Dvornic, P.R., 2009. Dendritic Polymer Networks: A New Class of Nano-Domained Environmentally Benign Antifouling Coatings. ACS symposium series 1022, 165–186. https://doi.org/10.1021/bk-2009-1022.ch011
Schloss, P.D., Westcott, S.L., Ryabin, T., Hall, J.R., Hartmann, M., Hollister, E.B., Lesniewski, R.A., Oakley, B.B., Parks, D.H., Robinson, C.J., 2009. Introducing mothur: open-source, platform-independent, community-supported software for describing and comparing microbial communities. Applied and environmental microbiology 75, 7537–7541. https://doi.org/10.1128/AEM.01541-09
Sciuto, K., Moschin, E., Moro, I., 2017. Cryptic Cyanobacterial Diversity in the Giant Cave (Trieste, Italy): The New Genus Timaviella (Leptolyngbyaceae). crya 38, 285–323. https://doi.org/10.7872/crya/v38.iss4.2017.285
Stanaszek-Tomal, E., 2020. Environmental Factors Causing the Development of Microorganisms on the Surfaces of National Cultural Monuments Made of Mineral Building Materials—Review. Coatings 10, 1203. https://doi.org/10.3390/coatings10121203
Sun, Z., Zhang, Y., Sun, L., Liu, J., 2019. Light Elicits Astaxanthin Biosynthesis and Accumulation in the Fermented Ultrahigh-Density Chlorella zofinginesis. J. Agric. Food Chem. 67, 5579–5586. https://doi.org/10.1021/acs.jafc.9b01176

Thompson, J.D., Gibson, T.J., Higgins, D.G., 2002. Multiple sequence alignment using ClustalW and ClustalX. Current protocols in bioinformatics / editoral board, Andreas D. Baxevanis ... [et al.] Chapter 2. https://doi.org/10.1002/0471250953.bi0203s00

Tomczyk-Żak, K., Zielenkiewicz, U., 2016. Microbial Diversity in Caves. Geomicrobiology Journal 33, 20–38. https://doi.org/10.1080/01490451.2014.1003341

Urzì, C., De Leo, F., Bruno, L., Albertano, P., 2010. Microbial Diversity in Paleolithic Caves: A Study Case on the Phototrophic Biofilms of the Cave of Bats (Zuheros, Spain). Microb Ecol 60, 116–129. https://doi.org/10.1007/s00248-010-9710-x

Větrovský, T., Baldrian, P., 2013. The Variability of the 16S rRNA Gene in Bacterial Genomes and Its Consequences for Bacterial Community Analyses. PLOS ONE 8, e57923. https://doi.org/10.1371/journal.pone.0057923

Warscheid, Th., Braams, J., 2000. Biodeterioration of stone: a review. International Biodeterioration & Biodegradation 46, 343–368. https://doi.org/10.1016/S0964-8305(00)00109-8

Wellburn, R.W., 1994. The spectral determination of chlorophylls a and b, as well as total carotenoids, using various solvents with spectrophotometers of different resolution. Journal of plant physiology 144, 307–313. https://doi.org/10.1016/S0176-1617(11)81192-2

Westcott, S.L., Schloss, P.D., 2017. OptiClust, an improved method for assigning amplicon-based sequence data to operational taxonomic units. MSphere 2, e00073-17. https://doi.org/10.1128/mSphereDirect.00073-17

Wickham, H., 2009. ggplot2: Elegant Graphics for Data Analysis. https://github.com/tidyverse/ggplot2.